Carbon Fiber Composites

Team Members: Vincent D'Angelo, Leo Georgopoulos, Zachary Martin, Christian Williams

Abstract

In vehicle competitions, success is defined by optimization. Teams work over months and years to iterate and optimize all systems of their vehicle to ensure the highest achievable velocity while expending the least amount of energy. One of the most straightforward and impactful methods of achieving this is through the reduction of vehicle weight, which lowers the energy cost for accelerating and maintaining speed. Here we design carbon fiber (CF) sandwich panels, or honeycomb aramid paper (Nomex) sandwiched between CF layers, for use in the structural design of these cars, especially for wing support and suspension applications as a replacement for traditionally steel and aluminum parts. These materials are far less dense than metal and offer comparable or improved performance, the trade-off being that the material system and processing is far more complex. In our design process, we observe the effects of different curing temperature profiles and amount of carbon fiber plies on select thermal properties, void size and density, and the strength of carbon fiber in tension and bending. These curing processes are designed with the goal of minimizing the presence of defects and maximizing the degree of cure (and thus epoxy molecular weight). The effects of features such as defects and other stress concentrators are analyzed through modeling with well-known materials physics equations. Additionally, we study the effect of drilling a thru-hole, similar to those used to mount CF sandwich panels, on the structure and tensile properties of the material. The end target of our investigation is to deliver optimized design criterion for CF sandwich panel construction which can be utilized by both the Formula and Solar teams here at Northwestern.

Introduction

Two of Northwestern's vehicle teams, NUsolar and NU Formula, regularly utilize carbon fiber for structural vehicle components, ranging

from external wing supports to a complete aeroshell to support an onboard solar array (Figure 1(a),(b)). As a lightweight, stiff, and high yield strength material, carbon fiber is a desirable substitute for traditional materials that can reduce vehicle weight and significantly improve race performance. The unavoidable issue of incorporating CF into a design, however, is that the composite is a far more complex material system that creates uncertainties in design safety factors and demands precise processing conditions in order to achieve performance comparable to manufacturer figures. These drawbacks are not an abstraction, but an issue the teams have painful history with, including an entire generation of solar vehicle (SC6) which was shelved after experiencing catastrophic failure of its structural CF during brake testing prior to a track race (Figure 1(c)).

Figure 1: Carbon fiber integration into team vehicles. (a) Wing, (b) Aeroshell, (c) CF panel failure at bolt connection with suspension system..

Another effect of switching away from a bulk material, such as a metal, is highly anisotropic behavior. This anisotropy causes the material properties to be far more sensitive to disruptions within the fiber layers and highly dependent on the direction of loading. As structural mounts for suspension components and airfoils within a vehicle, these components are expected to handle a variety of known and unknown stresses, and therefore quantitave performance data must be available for the material in a large number of loading conditions for safe implementation.

Additionally, the process to mount CF components into a larger vehicle system will create a thru hole in the component that introduces local-

ized delamination of layers and acts as a geometric stress concentrator. As such, non-ideal composite panels are inherent to vehicle applications, and an investigation that identifies how these defects alter the mechanical performance of composite sandwich panels is essential. In this design project, we apply the materials science paradigm to build a connection between underlying microstructure and the macroscopic effects it has on parts fabricated by our vehicle teams. This process also extends beyond analysis to emphasize optimization, identifying variables within the system that can be altered to minimize defects and voids in the final CF resin matrix.

This allows our project to provide not only a more accurate quantification of carbon fiber performance, but also deliver an optimized design criterion that can be utilized by both NUFSAE and NUsolar to fabricate better parts moving forward. We further emphasize this goal of an immediately implementable outcome by attempting to achieve an optimal performance using processing techniques and equipment that our teams have previous experience and available funding to work with.

The variable of interest in this optimization effort is the temperature profile used during the CF curing process. It has been shown that an important method for tuning the properties of CF is the delay of matrix gelation, which occurs as a function of extent of reaction [1, 2]. Certain temperature profiles can increase the processing window for the material and allow the diffusion of defects, such as voids, to take place over longer periods of time due to the resin maintaining a lower viscosity until later in the curing process. Since these voids cannot support loads, if frozen into the final matrix they act as stress concentrators that reduce the fracture toughness and strength of the macroscopic material. Our design process investigates three temperature profiles from previous literature, which were adapted to the specific material and equipment setup available to the NUFSAE team and used to prepare sets of CF samples of varying dimensionality and ply number [1]. Various methods are then used to characterize these samples and modeling based on well-known materials physics equations is employed to better understand our observations.

The choice to approach this system from an experimental perspective is due to the issues associated with computational modeling of the entire carbon fiber-epoxy-Loctite-Nomex system. This process is intensive, difficult, and highly dependent on the reproducibility of raw materials and processing conditions to match the model. However, as previously

demonstrated a clear understanding of carbon fiber performance in relevant loading conditions is necessary for proper incorporation of the material into vehicle design. By identifying the key variables in the processing, structure, and performance, we therefore reduce the variables within the system to fit the scope of a physical investigation, which can provide experimental results immediately available to the benefit of each team. Specifically, by learning the ultimate mechanical performance of the material (made with available processing equipment), how performance is altered by the introduction of necessary stress concentrators (i.e. a bolt), and how the curing profile can be altered to improve final microstructure and mechanical performance, each team can be provided the values and methods required to more successfully design and manufacture the material. This work also represents a significant risk minimization step for both organizations, preventing lengthy redesign processes by design and manufacturing teams while minimizing the loss of capital associated with part failure.

System Design Chart

In this project we perform an in-depth investigation of the impact of processing conditions on the structure, properties, and final performance of the CF-Loctite-Nomex system for use by both Northwestern Solar and Formula. This emphasis on initial processing is rooted in our desire to deliver an optimized system team engineers can feasibly control, as members can readily alter how CF is cured, but lack the capabilities and background to capitalize on other materials level alterations. This is made further relevant by each team's decision to purchase preinfused resin composite matrices, which eliminates control over these variables unless switching product manufacturers.

Since the integration of CF becomes desirable to our vehicle teams only when it offers high performance and weight-saving potential, mechanical performance serves as the motivation behind every other consideration on the design chart we investigate. The complexity of the CF system – a multi-component structure with highly anisotropic properties and a large number of changeable processing conditions – also demands that we define a clear scope for our analysis within the larger materials design space. We therefore emphasize the variables that connect directly from mechanical performance to initial processing, and as

demonstrated in Figure 2 below, these desirable properties are intertwined with many structural characteristics of the system.

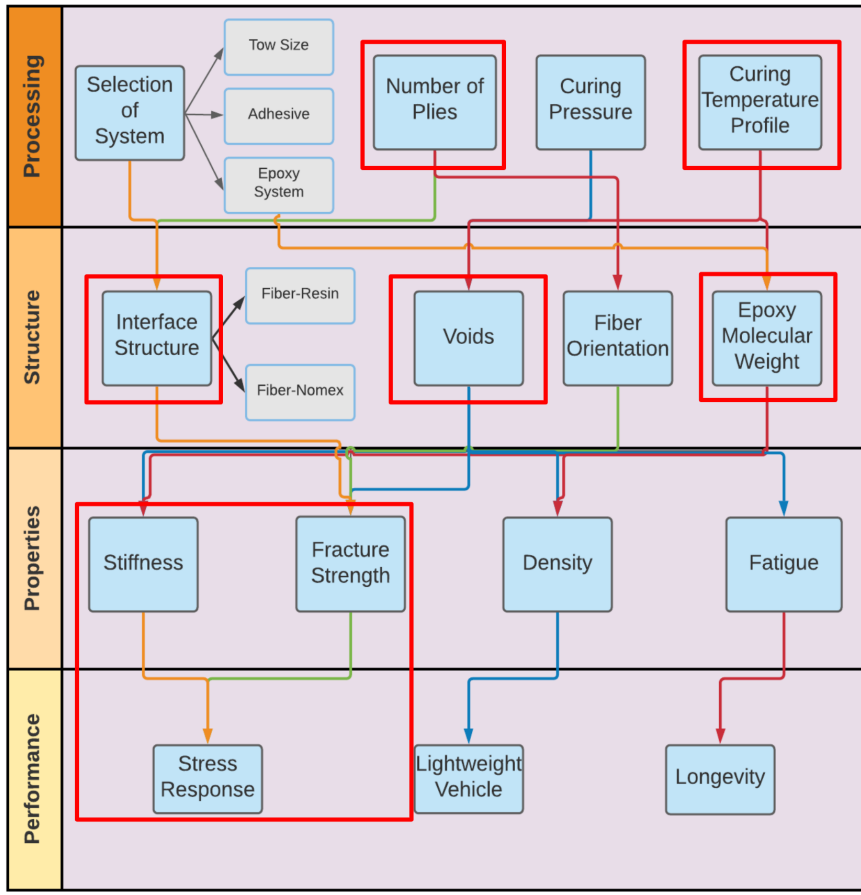

Figure 2: System design chart. The focuses of our investigation are highlighted with red boxes.

Key structural features such as the CF-Loctite-Nomex interfaces will directly affect the mechanical strength of the final panels, and introduce an entirely new set of possible failure modes to the larger system. Other variables, such as the orientation of the carbon fiber sheets, also significantly affect directional performance, although its geometry is standardized throughout much of the industry to maximize isotropic behavior. Other important structural variables are microscopic defects that can aggregate into macroscopic voids, as well as the molecular

weight of the epoxy, which is dependent on curing conditions. These affect ultimate yield stress and material stiffness, respectively, and are therefore major considerations in the optimization process. Observations on these structural features can be conducted through both optical and thermal methods.

We specifically focus on the impact of interface structure, void content, and epoxy molecular weight as key characteristics that are heavily controlled by processing, and have significant impacts on the desired mechanical performance metrics. By varying curing temperature profile in initial processing, we can alter the extent of reaction and final microstructure achieved, which impacts two variables significant to the vehicle teams: the elastic modulus and failure stress of the material. Evaluation of panel performance is done through tensile and bend testing to confirm the maximum stresses these panels can support without fracture, and identify for what applications they can be employed within the cars.

In all, building a holistic understanding of how these pieces of the design paradigm interlock promotes a deeper understanding of where macroscopic performance changes originate, and opens the door to further optimization and quantification of the CF system's materials properties. Our dual-pronged approach on different length scales capitalizes on the connections between microscopic matrix evolution due to processing and final performance, while making it clear on a materials level how to design and implement improved processing conditions.

Materials Selection

For many automotive applications, steel and aluminum based alloys are highly desirable for their workability and low cost. In most commercial models, aluminum chassis serve as the backbone of the vehicle, providing the necessary mechanical strength while being light enough to ensure acceptable fuel efficiency. However, for performance applications where speed or long term endurance is required, further materials optimization is necessary to create a competitive vehicle. The primary driving force behind this optimization effort is the goal of reducing vehicle mass, as using simple Newtonian physics we can show that the force required to drive acceleration is directly related to the mass of the object in question.

$$F = ma$$

In a track competition, the cycle of acceleration and deceleration occurs on each bend of the road, and makes this relevant countless times throughout the course of a race. Looking at another application, the solar vehicle operates mostly on open roads, but mass remains a relevant factor due to the restorative drag forces acting on the vehicle, which requires constant acceleration to counteract.

For these reasons, professional manufacturers and our university's teams alike turn to alternative structural materials capable of preserving the high mechanical performance of bulk metals, but with lower densities that allow for higher performance. The effects of this effort cannot be overstated, and represent a meaningful variable in maximizing vehicle acceleration and endurance.

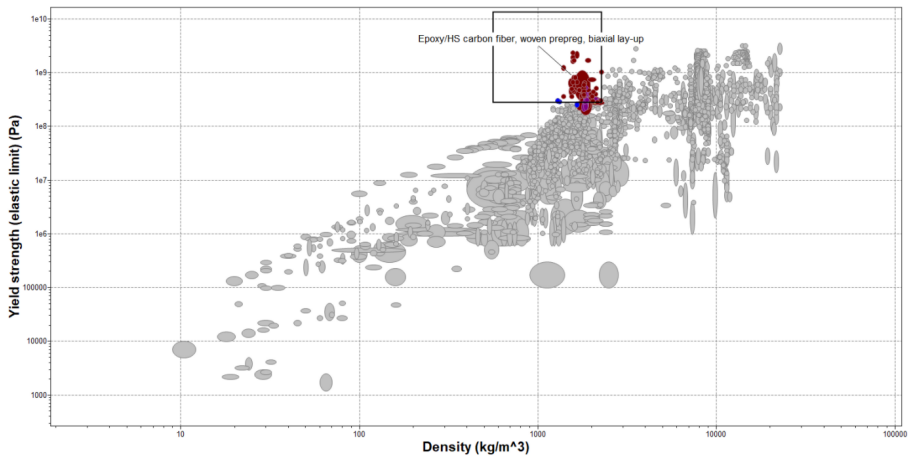

Figure 3: Ashby plot of yield strength vs. density. Max calculated von Mises stress on the wing support with a safety factor of 2 is the lower bound on yield strength

The first properties considered were yield strength and density, as the overarching goal was to create a structural support that that reduces vehicle weight while maintaining sufficient mechanical performance. An inclusion criterion was manufactured to filter suitable materials, with the lower bound on acceptable yield strength performance derived from a previous application of FEA to the formula vehicle, which

identified a maximum von Mises stress of 1.3778E+8 N/m^2 on the vehicle wing. To ensure long term durability even in extreme conditions, a safety factor of N = 2 is applied to this value, setting the minimal benchmark at 2.7556E+8 N/m^2. On the other axis, density is bounded by an upper limit by lightweight metals like aluminum, such that anything within the zone of interest will represent an improvement over current solutions. Carbon fiber composites perform very well in the density vs yield stress analysis, being stronger than metals like low Carbon steels and aluminum while remaining less dense (Figure 3). Furthermore, the integration of a sandwich panel construction allows for this support to be rigid in the transverse direction and even more lightweight, due to the ultra-low density Nomex within the core. While carbon fiber composites are less easily workable than these bulk materials, the low scale of production in the context of the car teams reduces the influence of this factor.

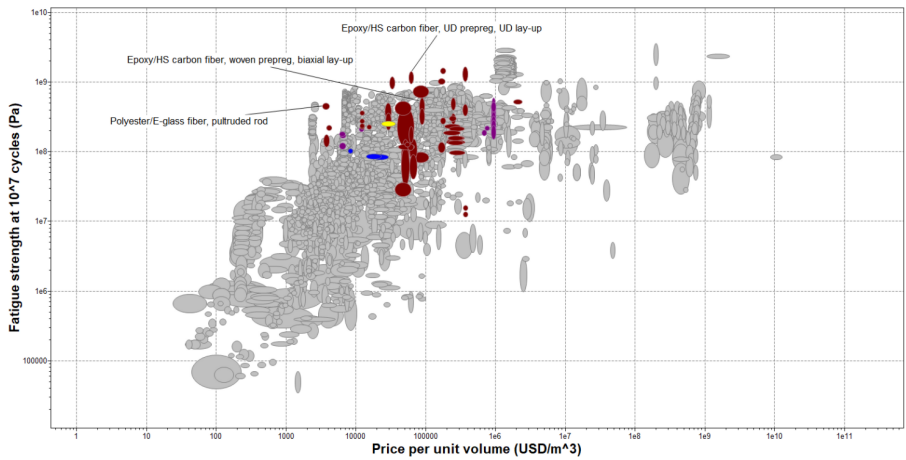

Figure 4: Ashby plot of fatigue strength at 10^7 cycles vs price per unit volume, after selecting for yield strength and density.

Next, longevity was considered. Fatigue strength is a major determinant in material failure over long time spans, and is highly relevant to our vehicle teams as supports experience constant stress from the weight of the parts it supports, as well as cyclical stress from the force of the air on the wing as the car accelerates and decelerates. After selecting using yield strength and density, few materials are left in the Granta Edupack database. Of these remaining materials, composite materials

are some of the best in terms of fatigue performance while undercutting the price per unit volume of many comparable materials (Figure 4). Longevity is a performance criterion that factors heavily into cost, as a measure of how often a part will need to be replaced. Since carbon fiber can meet longevity demands while maintaining an acceptable cost, it is a good fit for this application.

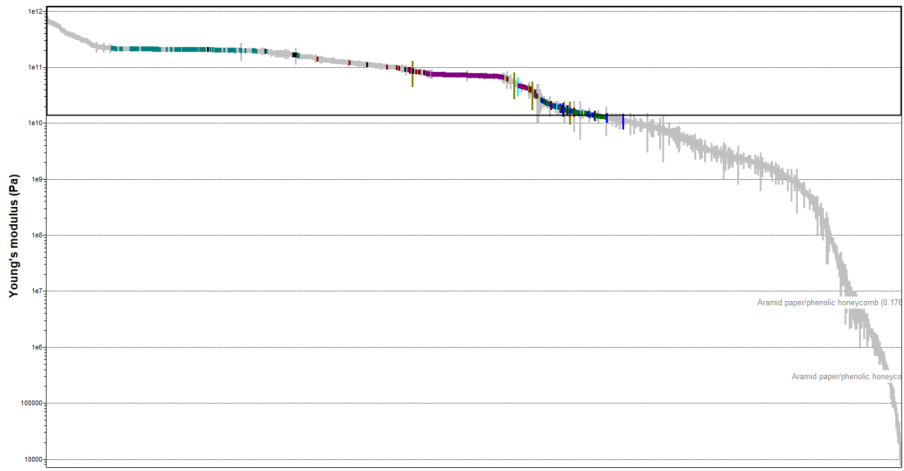

Figure 5: Young's modulus for a range of materials.

Finally, we investigate the elastic moduli of our materials to ensure sufficient stiffness for structural or external applications (Figure 5). Whether a windfoil or part of a monocoque chassis, the ability to maintain shape and dimensionality under applied stress is critical to feasible implementation into a complex and tightly designed vehicle. Warping can lead to performance reductions as a result of worse aerodynamic structure, or to more critical failures such as the bending of the solar array on the upper aeroshell of the solar vehicle. Previous iterations of the team vehicle have successfully implemented more traditional metals in this application, so we use this as a benchmark a replacement material must approach. Once again, we find that carbon fiber outperforms previous used materials, and offers a higher stiffness and thus better dimensional stability under loading.

As carbon fiber is able to meet or exceed all of the relevant criterion, we justify the use of the material for application in structural components by our vehicle teams. Furthermore, the significant performance

increases derived from its material properties represent a powerful tool for both NUFSAE and NUsolar, and providing the methods and information necessary to further integrate it into the design process is critical to the competitiveness of both organizations.

Design Strategy

Composite matrices represent a complex material system with performance highly dependent on processing, machining, and force loading conditions. This design project is an investigation of the behavior of a carbon fiber matrix for use in a vehicle system, applying a microstructural analysis to the observed mechanical performance in order to facilitate the optimization of processing and machining conditions employed by Northwestern's FSAE and NUsolar teams. This process can also validate whether a carbon fiber-based material can survive the maximum forces expected in operation, demonstrating the conditions in which it can be used as a structural support. Sandwich panel construction further bolsters the impact of our analysis, as the demonstration of adequate performance in this form allows for the integration of a very low density material to reduce vehicle weight.

Our design process focuses on the relationship between processing and mechanical properties by analyzing the effects of different layup parameters and curing temperature profiles. Failure of carbon fiber composites often occurs when stresses exceed the maximum yield strength of the individual fibers or of the fiber-matrix interface. However, in the case of the sandwich panels there are additional interfaces to consider: the CF-Loctite and Loctite-Nomex interfaces. This special consideration for our system is critical in our design considerations and characterization. The product of the design effort will be an assessment of the validity of the sandwich panels, especially in light of this new failure mode, and initial optimization of processing conditions. The 3 curing temperature profiles used were adapted from relevant literature [1, 3] in order to compare the impact of processing conditions on the final properties of the carbon fiber, with special emphasis on the comparison of the relative void contents (Figure 6). These temperature profiles were scaled down to fit the curing temperature of our available carbon fiber, which cures below the temperature of the material used in the comparison literature. All proportions are retained, but instead peak at a maximum

275° F, the temperature recommended by the manufacturer. Number of plies were only varied for samples in the Standard Curve.

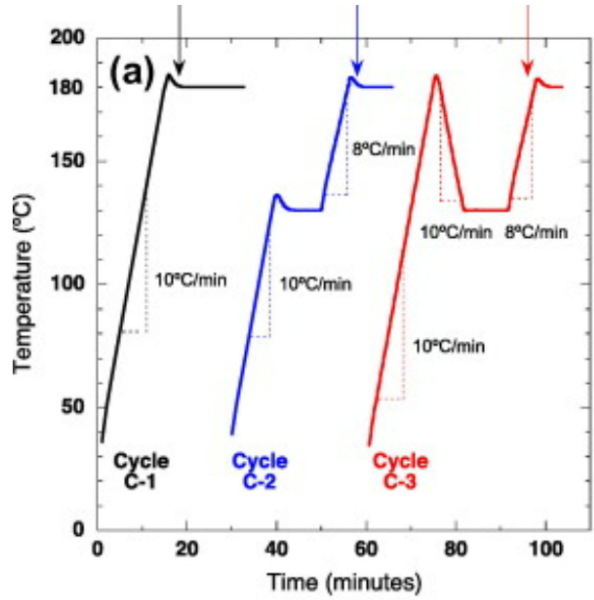

Figure 6: Curing curves adapted for our design. (black) Standard Curve, (blue) Hold Curve, (red) Dip Curve. [1]

Our characterization strategy is four-pronged, and combines the use of modeling with well-known materials physics equations with thermal, mechanical and optical analysis of prepared samples. Through this process, we are able to investigate systems of different scope and qualify observed performance within the context of modeled stress concentrators and real microstructure. The techniques used to extract the relevant material and system features are: tensile and bend testing, optical microscopy, differential scanning calorimetry (DSC), and modeling using equations for diffusion and stress concentration. In the cases of both tensile testing and optical microscopy, the effects of a drilled hole on the structure and mechanical properties are observed, modeling a feature present in carbon fiber panels used by both the FSAE and NUsolar teams.

Bend testing is performed in order to quantify the strength of sandwich panels without the influence of a drill hole and to analyze the strength of the internal materials of the panel construction. Tensile testing per-

formed by loading at a bolt allow for the measurement of the panel's Young's modulus and yield strength under a realistic loading condition, providing insight into mechanical feasibility and longevity. The inclusion of this stress concentrator is significant because a bolt hole will be present in every piece mounted for structural application.

DSC characterization acts as a way to determine the degree of cure for carbon fiber samples across different curing temperature profiles. The degree of cure is an important parameter that directly relates to extent of reaction, epoxy molecular weight, and thus material stiffness or elastic modulus.

The features visible through optical microscopy are especially relevant to mechanical behavior. Cross-sectional images of the CF-Loctite-Nomex architecture cured with each temperature profile are captured of in order to observe the vacancy concentration in the CF from each cure. Images were also captured of the microstructure after a hole was drilled into a panel in order to make conclusions about stress distribution near this necessary macroscopic defect. Disruption and chipping around these holes makes it difficult for stresses to be distributed throughout the material, and an analysis of this damage is therefore significant to performance predictions. In tandem, these two interface analyses allow us to better understand how curing profile and manufacturing directly impact vacancy concentration and stress concentrators within the CF panel, further corroborating the mechanical properties observed in tensile testing.

Throughout our design process, all members worked together on synthesis and processing. DSC was headed by Christian Williams, microscopy by Leo Georgopoulos, and mechanical testing by Zachary Martin and Vince D'Angelo.

Materials Modeling

As discussed previously, the NUsolar and NU Formula teams do not use CF sandwich panels alone as structural components. As a part of a larger vehicle system, each team drills holes into the material to connect the panels to components such as the suspension, aeroshell, wing, etc. In addition to disrupting the carbon fiber weave, the results of this create a geometric stress concentrator within the sample that amplifies the load experienced in the region nearby. This is due to the inability of

voids to support loads, which intensifies the stress on nearby parts of the matrix to compensate.

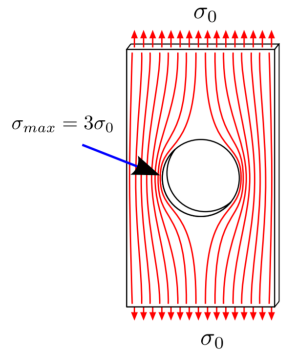

Figure 7: Concentration of stress lines around a circular hole in a material bulk.

The geometric effects of this stress concentrator can be quantified using the crack and stress intensity factor models, and additional corrections can be made to explain the impact of CF weave delamination and processing errors. The most general effects can be derived from the macroscopic dimensions of a bolt hole, with exact concentration dependent on the ratio of the major and minor axes of the ellipse [4]. As our bolt holes are circular in nature ($a_c = b_c$), the following equation for geometric stress concentration simplifies to be a constant factor of 3.

$$\sigma_{max} = \sigma_0 \left(1 + 2\frac{a_c}{b_c}\right)$$

The effects of delamination and processing errors are more difficult to quantify, but both can be represented as a stress intensity factor (K) that results in part failure before what is expected in previous literature and Granta Edupack.

$$\sigma_{max} = \sigma_{failure} = 3\sigma_0 * \kappa_{delamination} * \kappa_{processing\ failures}$$

Using sandwich panels requires another important physical model, the neutral axis, to be considered when predicting local stresses within the

larger architecture. As shown in Figure 8, when a beam is in bending, one face of the beam will be subjected to compressive stress, while the other is subjected to tensile stress. For a perfectly symmetrical beam these will be equal and opposite, such that a neutral axis exists within the core at which there will be no longitudinal stresses. The operating principle of CF sandwich panels is very similar to an I-Beam, wherein that cured CF is very strong and can support the high stresses at the surface, while the low density, weaker material (Nomex) can withstand the smaller stresses at the center of the panel.

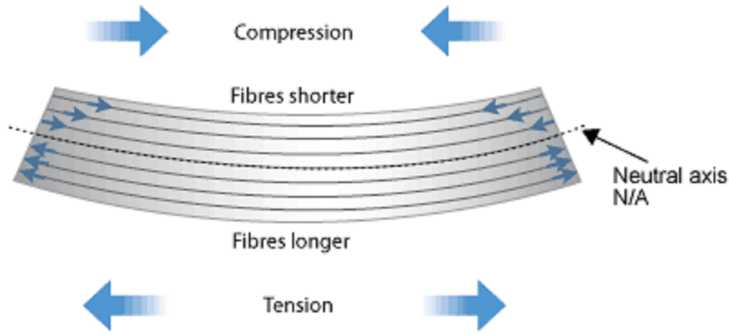

Figure 8: Concentration of stress lines in a beam in pure bending.

Another important interaction within our system occurs during the initial curing step, and is responsible for our investigation of several curing profiles. When working with pre-impregnated (prepreg) carbon fiber, the epoxy resin is already deposited throughout the carbon weave, but also present in the uncured bulk are undesirable vacancies and larger voids which act as stress concentrators, similar to the larger bolt hole previously discussed. Since carbon fiber is a brittle material these voids present a significant issue, as failure in the bulk will occur at the largest of these defects [4]. Therefore, to minimize the adverse affect of voids on the final material, it is possible to exploit the temperature dependent behavior of diffusion kinetics and the activation barrier of the curing reaction. Focusing first on how voids can be removed from the bulk, the vacuum created in the manufacturing process creates a pressure gradient flowing down from within the sample. This provides a driving force to promote vacancy motion towards the surface of the sample, at which they exit the system. Unlike assumptions made in previous materials science courses, volume is not constant throughout this process and the exiting voids are not replaced by another defect. In-

stead, the material undergoes slight dimensional shrinkage during this interaction.

However, the kinetics of the diffusive movement of vacancies follows Arrhenius behavior, and as such this cannot be completed on a reasonable time scale at room temperature [9]. Following the temperature dependent diffusion relation, we observe that holding the system at a higher temperature will exponentially decrease the time scale required for meaningful void diffusion, but it is also important to consider that our composite material begins its curing reaction at 135° C. [3]. A final consideration to make is the microstructure surrounding the vacancies. Prior to curing the system is soft and made of polymer precursors. By heating the system, we are also increasing chain mobility which further decreases the energy barrier to void diffusion below that expected in a crystalline lattice. By investigating curing profiles that hold the system at an elevated temperature below the critical curing point, we can maximize the rate of void diffusion out of the material bulk while preventing the transition of the system to a stiff gel that prevents almost all void diffusion.

$$D^* = D_o \exp\left(-\frac{Q}{RT}\right)$$

Figure 9: The arrhenius relation for diffusion.

In order to quantify the transition of the epoxy system from the uncured resin to a network polymer, we employ a metric called the degree of cure. The curing reaction for epoxy is exothermic, and as such thermal methods can be used to analyze the progress of the curing reaction. A previously cured sample can be analyzed by DSC to measure the amount of heat released over time as a function of temperature. This residual curing enthalpy can be normalized to the curing enthalpy of a raw prepreg sample to extract a degree of cure associated with the extent of the epoxy reaction. The degree of cure, based on heat flow from the reaction, allows us to make a quantitative conclusion about the extent of reaction of the epoxy matrix. This value relates directly to the molecular weight of the polymer matrix as well as the crosslinking density, from which the strength of the matrix is derived.

$$\alpha = 1 - \frac{\Delta H_{res}}{\Delta H_{total}}$$

Processing

The procedures used to create our samples were taken from the car teams' past documentation and modified to suit our specific needs. The processing of carbon fiber has been refined over the course of decades by both academics and industry professionals; however, these methods cannot be replicated by the car teams as they have limited access to professional equipment, specifically autoclaves. The typical method of creating carbon fiber parts using preinfused matrix systems involves vacuum sealing a carbon fiber sheet and its mold inside a specially made bag, placing it in an autoclave, then controlling the temperature and pressure as indicated by the manufacturer. A significant challenge for the car teams is nearly all manufacturer's curing profiles require simultaneous and precise control of both pressure and temperature, as shown in Figure 10. Temperature control is important due to its influence on the gelation time of the resin matrix, while pressure control is important as the pressure differential between the vacuum sealed part and the ambient environment is the driving force for void diffusion out of the matrix. Due to cost constraints, the method provided by the teams allows for very limited control of both the temperature and pressure differential during manufacturing.

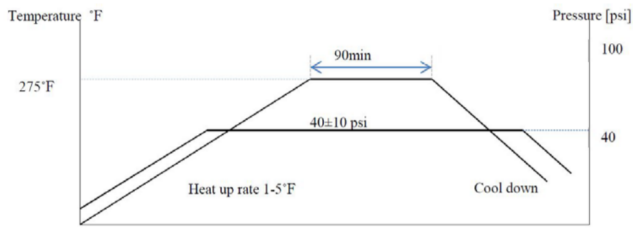

Figure 10: Manufacturer's recommended curing curve for our resin system.

In order to understand our rationale behind various changes, we will first outline the overall manufacturing procedure used by the car teams to cure prepreg CF. First, the proper number of plies of CF are cut in alternating 0° and 45° directions and placed over one another. At this

point, the resin system is tacky and various particles can adhere to the CF so great care must be made to prevent contamination of the system and bunching of the CF layers which may cause the system to improperly cure and delaminate where the layers stick to themselves as seen in Figure 11. Next, the mold is coated with a mold release or sheet of fabric to prevent the piece from curing directly to the mold and being impossible to remove. Once the CF is placed onto this layer of mold release, a layer of both peel-ply and breather are placed over it. The breather acts as a diffusive layer through which the air and volatile gases are removed from the entire CF part evenly. The peel-ply layer simply prevents the CF from sticking to the breather, which would ruin its surface finish. Finally. The entire mold is placed in a flexible, high-temperature, vacuum bag, which is sealed and has the air removed with a vacuum pump. The pressure inside the bag is brought to 0.3 ATM and then placed under an array of 500 Watt halogen lamps to activate the curing cycle for the resin system. Normally, the temperature of the CF is controlled by making an initial guess of the distance needed between the CF and halogen lamps to keep every part above the curing temperature then adjusting the positioning individual lamps once surface temperatures are read using an infrared temperature gun.

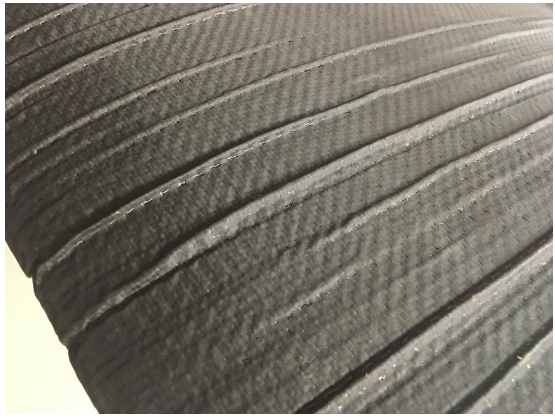

Figure 11: Dimples in a cured CF piece caused by poor placement of plies during the manufacturing process.

Our processing method was very similar to this with the exception of one key difference, we kept the position of each light on the heating array, shown in Figure 12, constant relative to one another throughout each cure while only changing the height of the overall array from the

curing CF. Eliminating all but one degree of freedom allowed us to better document our results as we found the necessary distances between the CF and lamp array to consistently keep the CF at both the hold and curing temperatures. We found that for a flat sample with a light array whose centers are placed 9.5 inches away from one another, a hold height 9.25 inches and 17.5 inches will keep the entirety of the sample above the curing temperature of 275° F and hold temperature of 200° F, respectively. When determining when in the curing cycle the array should be adjusted, we used the minimum temperature found on a piece of CF anywhere within the sample to determine when to start the hold timers for each curve as well as when to start the temperature dip for the third curing profile. This likely led to errors in our manufacturing, but it gave us a consistent procedure and ensured the entire sample was fully cured before removing it, a problem that has affected the car teams in the past.

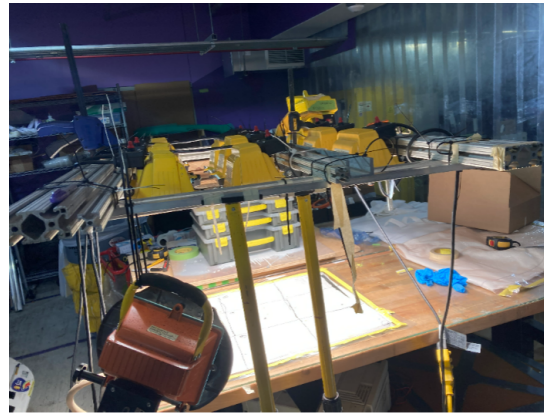

Figure 12: Lamp array setup used to cure our CF samples.

Along with the errors caused by our temperature metrics, there were several other potential sources of error within our manufacturing procedure. First, the lamps are held onto strips of metal with zip-ties and clamps. Any inaccuracy while securing the lamps can manifest by the lamps head not being parallel with the sample, which can significantly change the temperature profile of the of a sample. We believe this to be one the factors that caused the discrepancy between the hold and curing temperature profiles during the Hold Curve as seen in Figure 13. In addition, during the cure cycle, the zip-ties used to secure the lamps heat up past the onset of their glass transition temperature, leading to

the lamps slipping into a non-parallel position. The temperature profiles we found could also be slightly inaccurate as the readings from the IR temperature gun can change as it is heated, causing inaccurate measurements. Given the consistency of our average across cures at similar heights, we do not believe this was a major source of error. Finally, due to the radial spreading of electromagnetic waves from the lamps, significantly changing the height of the array can change the shape of the temperature profiles, which can be seen in Figure 13 as well. While each of these factors likely caused a degree of error within our measurements, we believe the consistency with which we used the minimum temperature metric, measured the distance between lamp centers when moving lights, and ensured the distance between the sample and lamp array was the same each time, all justify the validity of our results. In addition, these are the same metrics and factors that the teams use while optimizing their own individual curing processes and should be mirrored in our design.

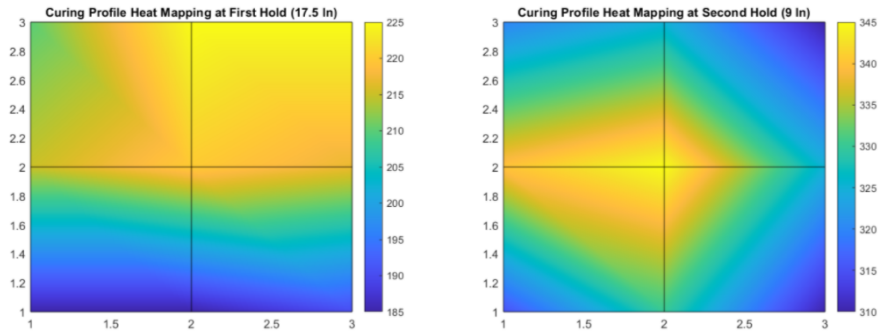

Figure 13: Temperature profiles from the 'hold' curing profile at the (a) Low temperature hold point and (b) Curing temperature hold point

Finally, once the CF was fully cured, we had to create the sandwich panels we would test. First, we used a CO_2 laser to slice the Nomex honeycomb into the correct sizes. Next, Loctite 9430 was applied to one side of the CF pieces and the Nomex was carefully put onto it. Weights were then placed on top of the Nomex as per the Loctite usage instructions and the pieces were left to dry for 24 hours. The process was then repeated for the piece of CF on the other side of each sandwich panel. Next, 1-inch squares of Garolite G-10 were applied to the samples that would undergo tensile testing using Loctite 9430 again. The alternate,

heat-based curing method wherein the adhesive was heated to 180° F for one hour was used as these tabs did not need to have as much resistance to shear stress. Finally, each sandwich panel was cut down to size using a pneumatic Dremel tool. This step eliminated any error created due to inaccurately placing the plies on top of one another before curing or while adhering them to the Nomex with Loctite. Then, for the bolt-testing samples a drill press with a speed of 3400 RPM with the smallest step size possible was used to create ¼ inch holes through the entire sample. Lastly, the optical microscopy samples were polished to allow for clearer imaging and better visibility of individual fibers.

Results

Determination of Extent of Reaction

DSC was applied to samples from each of our curing profiles and an uncured sample. The resulting heat flow curves of the pre-cured samples were then compared to the curves of the uncured samples in order to extract a degree of cure. Unexpectedly from prior literature [1], we observed no noticeable residual curing peaks within the cured samples (Figure 14).

This absence of residual curing peaks implies that each of our cures resulted in nearly the identical extents of reaction, with gelation ceasing as a result of the dilution of unreacted functional groups losing mobility within a stiffening matrix. This process vastly lowers the speed of the reaction process such that unreasonable time scales would be needed for further curing. This test has demonstrated that epoxy molecular weight is not varying significantly across different curing temperature profiles, and therefore places the emphasis of our investigation on void diffusion and the resulting microstructure, which may have locked at different time scales and trapped voids. This means that the thermal analysis does not rule out variations in void distribution. Thus, our DSC analysis allows us to interpret our mechanical and optical microscopy results without heavily considering the effects of different degrees of cure and epoxy molecular weights.

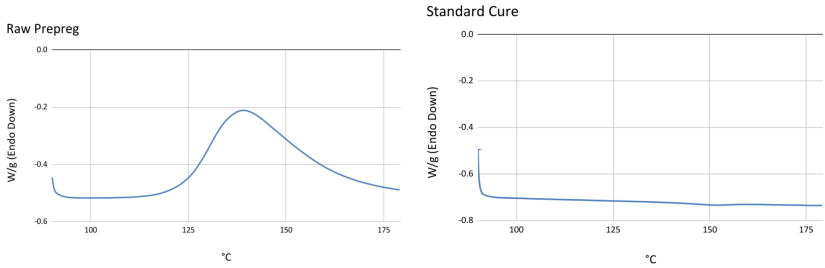

Figure 14: DSC curve for an uncured CF sample (top), DSC curve for the Standard Curve sample (bottom)

Glass transitions were anticipated to be seen in the thermal analysis. Since functional group mobility is needed for the curing reaction to progress, and the glass transition marks a transition to less mobile chains, the glass transition is expected to take place near the temperature at which the epoxy was cured. After performing a baseline correction on the data from the Standard Curve, a distinct endothermic peak was seen near 150 °C (Figure 15). It was concluded that this was due to an aging effect that became visible at the glass transition as an enthalpy overshoot peak. As a material is aged below its glass transition, it can reduce its enthalpy as it approaches the state represented by a decrease in enthalpy on-track with the heat capacity above the glass transition. When the glass transition is reached after aging, the relaxed matrix can overshoot the glass transition and absorb enthalpy proportional to the enthalpy released during aging (Figure 15). Since this endothermic event occurs near the temperature at which the matrix was cured, we conclude that this is a glass transition [2].

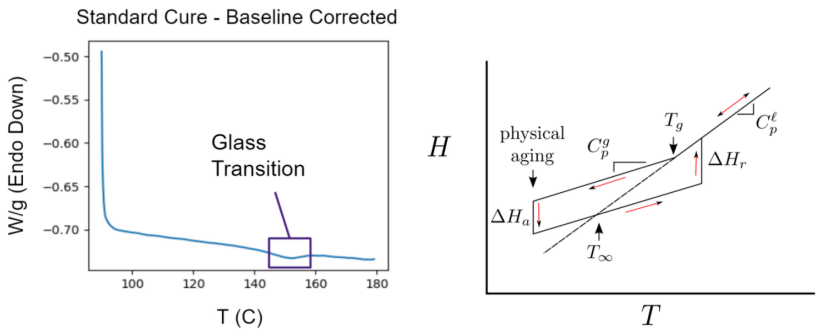

Figure 15: Baseline adjusted DSC curve for the Standard Curve (left). Schematic of glass transition hysteresis due to aging enthalpy (right)

Analysis of Void Distribution from Varying Cure Profile

After determining that all three cures led to epoxy networks with similar extents of reaction, we worked to calculate the void density and distribution from each profile to identify the effect of each curing profile on void diffusion. A Nikon optical microscope with adjustable objectives was used to image the cross-sectional area of the 0° CF-45° CF-Loctite-Nomex (orange, light blue, purple, and green respectively in the bottom image of [16]) interface, recording the void (red in the bottom image of [16]) density of the CF. Images were taken at a 10x magnification (top left image of [16]), and subsequently filtered in ImageJ to construct a binary image. Pixels with a brightness value below a certain threshold (i.e. voids) are assigned a value of 1, while those above (i.e. material cross-sections) are assigned a value of 0 (top right image of [16]).

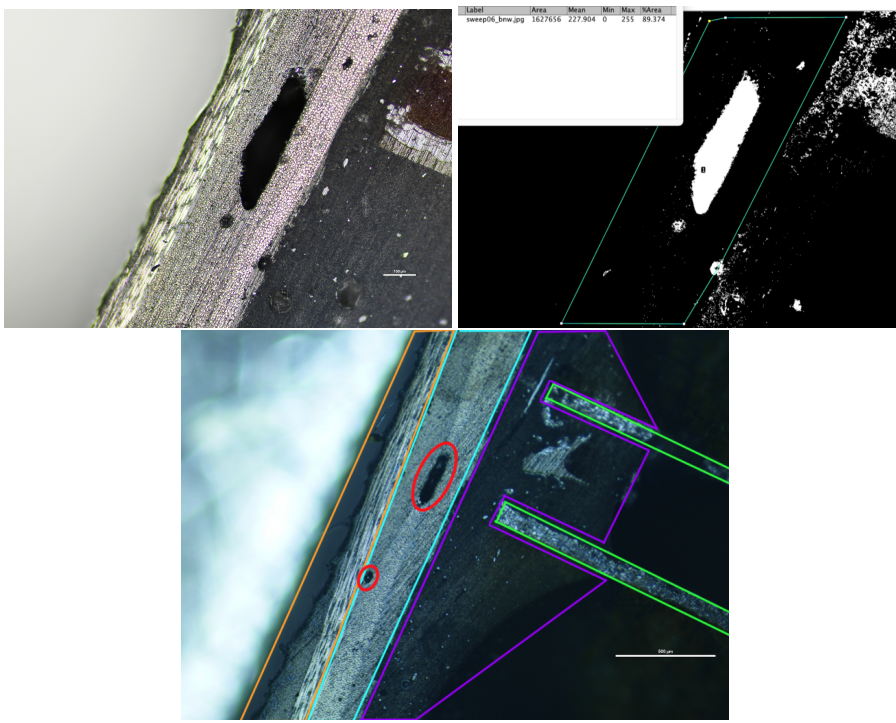

Figure 16: Sample optical image of the CF-Loctite-Nomex interface before ImageJ filtering (top left), ImageJ-filtered image highlighting relevant voids (top right), sample optical image of the 0° CF (orange) - 45° CF (light blue) - Loctite (purple) - Nomex (green) interface (bottom) .

Performing this systematically for 15-20 randomly chosen areas per curing profile, we calculated total void concentrations for each profile, as shown in [1]. Unsurprisingly, the Standard Heating Curve, which was expected to have the fastest gelation time, was the highest in void concentration at 4.77%. The Dip Curve was only 1% lower than the Standard Curve, and the Hold Curve was much lower than both at <1% concentration. This demonstrated that the Standard Curve induces the fastest gelation of all the curing profiles, while the Hold Curve delays gelation the longest. The Dip Curve, unlike previous literature demonstrated, resulted in comparable void fraction, and thus gelation time to the Standard Curve. This is an observation we associated with the rapid curing time of our resin and the much slower temperature decline achievable with the vehicle teams' heat lamp setup, which resulted in gelation during the initial heating step. As an inherent limitation of the curing equipment that both car teams use, this demonstrates that profiles that reach the curing temperature before quenching temperature are unfeasible for implementation.

Curing Curve	**Void Concentration**
Standard Heating	4.77%
Hold	0.89%
Dip	3.51%

Table 1: Carbon fiber void concentration from various curing curves

There were two major void types present within the Standard Heating and Dip Curves: (1) large voids along CF-CF interfaces and (2) small stream-like void patterns throughout a single CF bundle. We can eliminate creases in the CF-CF interface due to ineffective pasting as the source of these large voids ([17] top left, right rectangle) because the surface CF interface would then jut out ([17] top left, left rectangle) to compensate. This is not observed, and thus the large voids were determined to be a result of void diffusion kinetics within the matrix. Although large voids are the most impactful stress concentrators within the CF, the small streams of voids as shown in the top right of [17] also disrupt the ability of the matrix to distribute loads, negatively impacting the yield strength. As shown in the bottom of [17], the Hold Curve largely lacks these macroscopic void types; instead showing an incredibly pristine interface with point vacancies spread sparsely throughout. In all,

this analysis of void density and type suggests that the Hold Curve CF panels should exhibit superior mechanical strength to the other two samples.

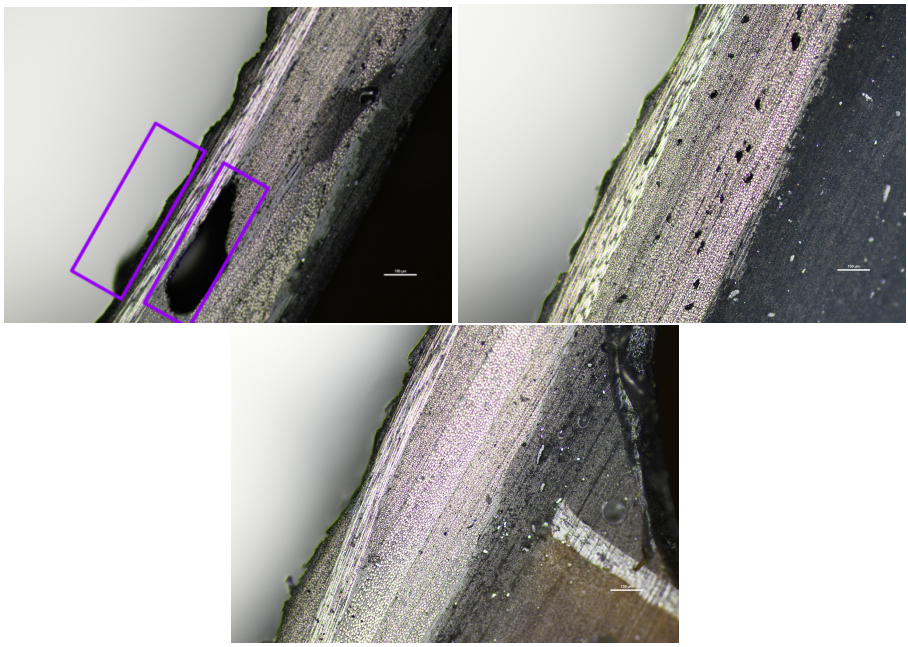

Figure 17: Sample image of large void with areas of note highlighted (top left), sample image of small stream-like voids (top right), sample Hold Curve image (bottom) .

Impact of Microstructural Optimization on Mechanical Performance

Previous sections have discussed the chemical structures and kinetic behaviors achieved through alteration of CF curing profile, and the resulting microstructures post-gelation. To connect this variation in microstructure to macroscopic part performance, we investigate the performance of constructed CF test samples under multiple loading conditions relevant to integration onto a vehicle. Specifically, we replicate two conditions: tensile loading at a bolt and stress induced under bending. The former replicates the most common method used to mount a structural CF panel to a larger vehicle system, and allows for the quantification of the stress each of these interfaces can support. The latter measurement is a less common, but still relevant mode that will pro-

vide insight into the stress response of the entire core structure to deformation. The results from these measurements will also reveal further information about the homogeneity between samples after both curing and post-processing, illustrating the significance of delamination of the CF matrix during drilling and the limits of the adhesive used at the CF-Nomex interface.

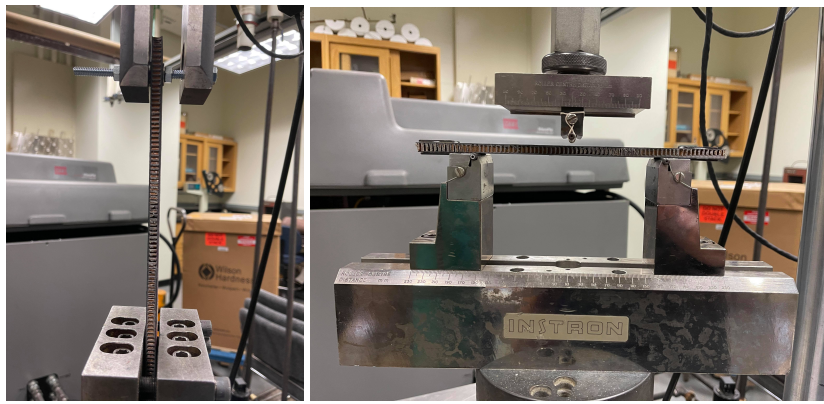

Figure 18: Mechanical testing methods employed. Bolt setup (left) and bend setup (right).

Looking first to loading at a stress concentrator within the material, we observed a gradual failure mode with plastic deformation occurring within the high compression region directly above the loading point. This corresponds to a local region of elevated stress concentration factor (K) such that the yield stress was exceeded in a small area of the sample, rather than across the entire cross-sectional area [4]. Examples of failed specimens are shown in Figure 19 below.

Figure 19: Bolt test parts after failure. Note the matrix failure localized to directly above the bolt.

Failure in these samples occurred significantly below the reported performance of CF in the Granta Edupack software as discussed in Materials Selection. This decrease in performance can be investigated in terms of the analytical model previously discussed, and the remaining decrease can be attributed to the delamination of the material, in addition to failure of the CF to reach industry performance values. Figure 20 below illustrates the absolute magnitude of the yield behavior for the Standard and the Hold Curve profile, which was previously identified to have the optimal microstructure. As highlighted in this Figure, the difference in yield stress between the Standard Curve (PXC2) and the Hold Curve profile (PXC3) is minimal.

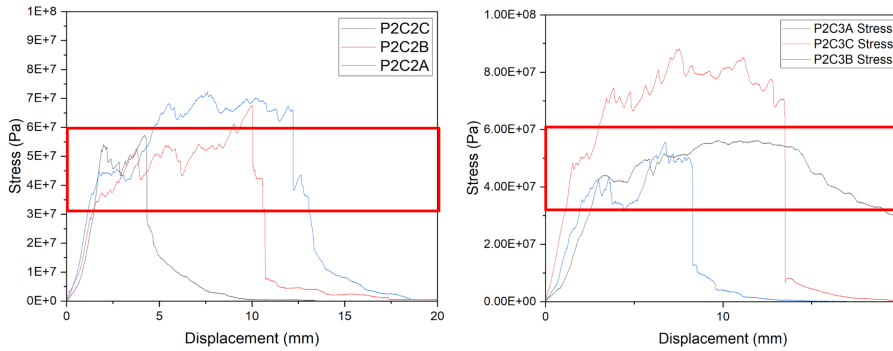

Figure 20: Stress v. Displacement plots for Standard (left) and Hold (right) Cures. Note the plastic failure regimes that exist when stress plateaus.

By comparing the behavior of each curve two important outcomes become clear: (1) only a small variation in failure stress is seen between the curing profiles, and (2) large variation in failure stress occurs within the curing profiles across each sample. This behavior demonstrates that yield stress under this loading condition is dominated by a sample specific variable, obscuring the impact of microstructural differences on the failure performance of these CF parts.

Looking at the effect of the number of ply on performance, we observe that there is a relationship between number of plies and initial failure stress, but that plastic deformation occurring after this initial break is highly variable. This reflects the impact of delamination on failure stress, as both microstructure variations and ply number become less impactful than the interface quality. We attribute this variation to delamination as this variable will shift significantly during this failure process due to the unpredictable weave destruction that occurs during the plastic failure regime (example images in Figure 21). In Figure 22 below, note the clear initial failure regimes for 1 (grey), 2 (blue), and 3 (red) ply specimens, and the subsequent large changes in yield stress afterwards.

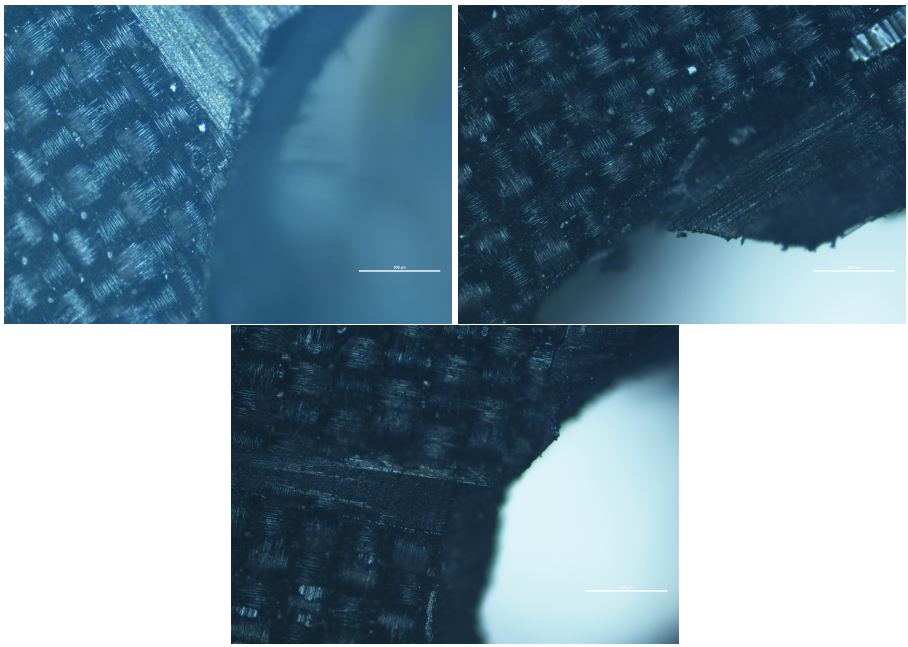

Figure 21: Sample delamination at drill hole edge.

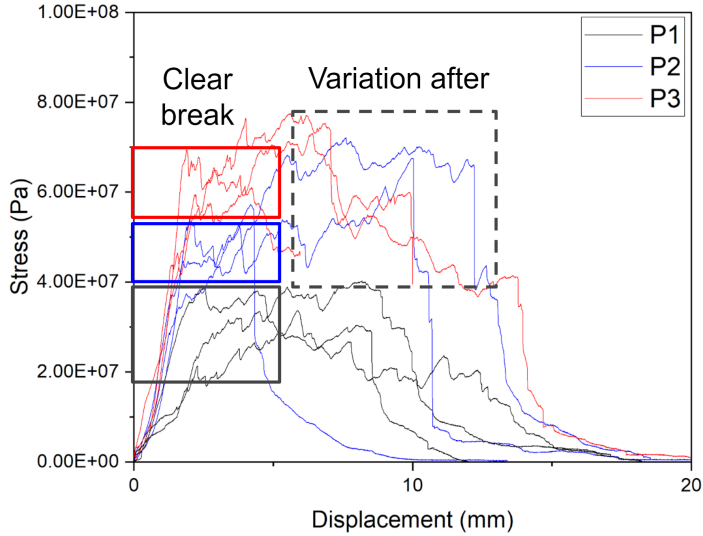

Figure 22: Stress v. Displacement plots for CF panels of varying ply number. Highlights added to illustrate tightly grouped initial failure stresses and large variation in behavior during uncontrolled plastic failure.

To isolate the cause of this variation in initial breaking stress observed within our sample sets, several specimens were trimmed and rerun using a more controlled processing environment. Previously created through the use of a hand drill, bolt holes through the standard and Hold Curve profile samples (dataset in Figure 19) were re-manufactured through the use of a mounted drill press to maximize control in interface quality. Previous literature demonstrates that delamination can be minimized through the use of a high RPM coupled with a small step size [5], which was implemented to greatly reduce the macroscopic damage at the interface. The results of this change are well reflected in the mechanical performance of these samples, which demonstrated a much tighter spread of initial failure. However, there is once again variation in performance after this point as the local delamination is uncontrollable after initial interface breakdown. After the elimination of variables from the testing process, a small increase in performance is visible in the Hold Curve samples relative to the Standard Curve profile. Figure 23 below demonstrates an average initial failure stress of 60 MPa for Hold Curve samples, compared to 52.5 MPa. For both sample sets, a much tighter spread of initial failure stresses is also visible.

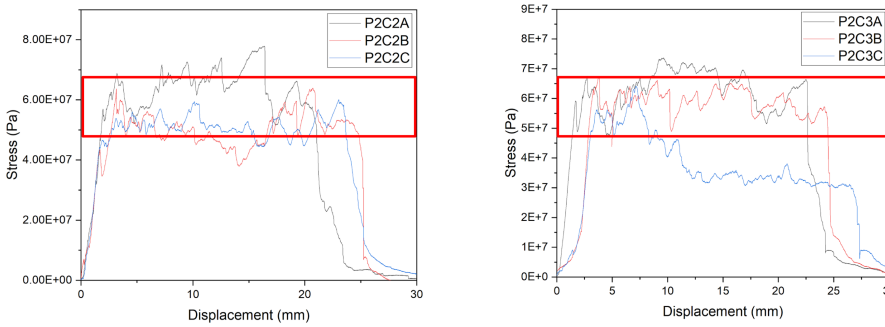

Figure 23: Stress v. Displacement plots for the Standard (left) and Hold (right) Cures with minimized delamination at bolt hole.

Analyzing sample behavior in the other loading condition, bend testing, we quantify the mechanical performance of the entire core structure and its interfaces under bending. This is due to the I-beam load distribution the core architecture exhibits, as illustrated in Figure 24 below, which will induce a force proportional to the distance a component is from the center of the material. This means the greatest loads are experienced at the CF outer interfaces, but also that the CF/Loctite/Nomex interface experiences a significant fraction of the maximum load.

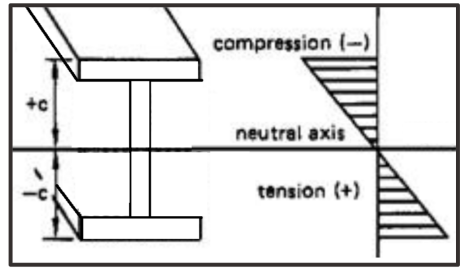

Figure 24: I Beam architecture, and the magnitude of compressive and tensile stresses throughout its cross-section.

Loading was designed to induce failure in 3-6 minutes, following ASTM standard D7250/D7250M [6], in order to separate the resulting failure mechanism from impact fracture. Unexpectedly, failure was not caused by failure of the CF exterior, but by delamination occurring between the CF and Nomex core. This process is a result of the adhesive failing, as neither the Nomex or CF demonstrate materials failure. This

mechanism occurred under an applied force consistently in the range of 250-300 N, and demonstrates an important data point for the vehicle teams to consider in the mechanical performance of their CF structural members. While available data for pristine systems may lead teams to believe they can support much larger loads, the processing and financial limitations of our teams prohibit the use of more expensive adhesives and thus parts used in bending modes must use this lower bound for failure, rather than the CFR performance.

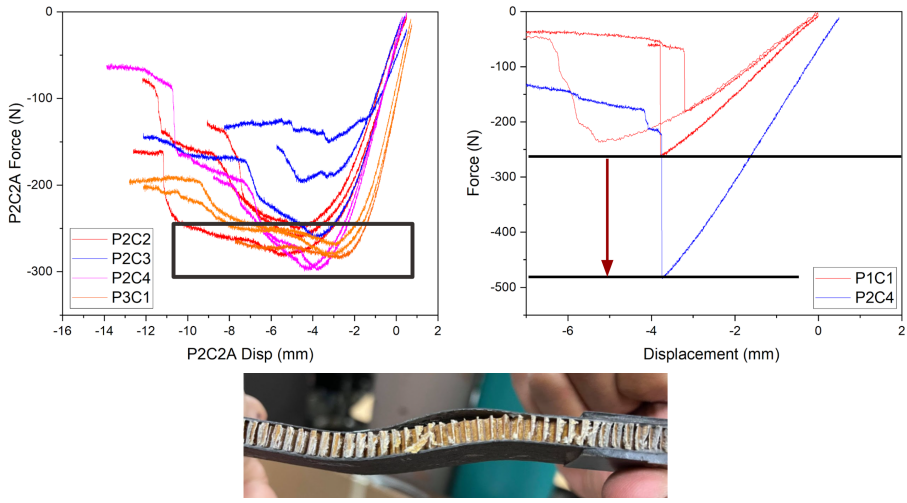

Figure 25: (top left) Bend testing plots of failure at the CF-Nomex interface. (top right) Bend testing plots of CF failure. (bottom) Image of CF-Nomex failure mode.

Of samples that did undergo failure in the CF regime, we see a clear correlation between number of plies and the maximum load supported before failure. The addition of a second ply approximately doubles the force necessary for failure, which occurs at a similar displacement / strain as the one ply samples.

The outcomes of this mechanical investigation have demonstrated that for several of the loading conditions relevant to the vehicle teams, performance is not limited by the CF matrix, but rather other components within the core architecture. The quantification of where these mechanisms lead to part failure will allow each team to better model CF in computational analysis, more accurately calculate part safety factors, and make preventative design decisions that prevent loading in these

fashions from occurring within structural CF components.

Conclusion

Our project is the first formal study conducted in conjunction with the student run car teams on Northwestern University campus to optimize the manufacturing techniques used for prepreg CF. Cost and time constraints prevent both teams from using techniques whose exact methodologies have been studied and published in research papers. While we did not directly compare the tensile strength of samples created with different curing profiles, we were able to confidently conclude that adding a low temperature hold at 200 F before ramping up to the curing temperature decreases both the size and frequency of voids in the cured CF. Voids are the main stress concentrators in CF composites as they are the largest defects present and consistently appear between plies. Thus, void density and size are good metrics for relative strength. DSC analysis showed there was no difference in the degree of cure between each curing profile, further strengthening the argument for the void content alone being a good measure of relative strength. In addition, we determined resistance to bolt-shearing was independent of curing profile and only significantly changed based on the number of plies used. The stress values and insight collected from these tests will be directly implemented into the design process of the car teams when considering CF sandwich panels for structural members. In addition, it was determined that the prominent failure mode in bending for sandwich panels with more than 1 ply on either side is delamination between the CF and Loctite layers. This will lead to an investigation into alternative methods for creating sandwich panels by the teams, and promote future studies of adhesive materials. Finally, the teams will extend our mechanical results to include tensile testing during the following quarters, capitalizing on the processing knowledge developed through this project.

References

[1] S. Hernández, F. Sket, C. González, J. LLorca, Optimization of curing cycle in carbon fiber-reinforced laminates: Void distribution and mechanical properties, Composites Science and Technology 85 (2013) 73–82. doi:https://doi.org/10.1016/j.compscitech.2013.06.005.

[2] Shull, K (2020). Soft Materials. Department of Material Science and Engineering Northwestern University.

[3] 14033-D, 2x2 Twill Woven Prepreg, Rock West Composites, San Diego, CA.

[4] Shull, K (2021). Mechanical Behavior of Materials. Department of Material Science and Engineering Northwestern University.

[5] O. Isbilir, E. Ghassemieh, Numerical investigation of the effects of drill geometry on drilling induced delamination of carbon fiber reinforced composites, Composite Structures 105 (2013) 126–133. doi:https://doi.org/10.1016/j.compstruct.2013.04.026.

[6] ASTM Standard D7250/D7250M, 2006 (2016), 'Standard Practice for Determining Sandwich Beam Flexural and Shear Stiffness', ASTM International, West Conshohocken, PA, 2016, DOI: $10.1520/D7250_D7250M - 16.www.astm.org$.